Available online at www.sciencedirect.com

ScienceDirect

Energy Procedia 142 (2017) 1736–1742

Energy Procedia

www.elsevier.com/locate/procedia

9th International Conference on Applied Energy, ICAE2017, 21-24 August 2017, Cardiff, UK

ORC cogeneration systems in waste-heat recovery applications

Oyeniyi A. Oyewunmi[a,*], Antonio M. Pantaleo[a,b], Christos N. Markides[a]

[a]Clean Energy Processes (CEP) Laboratory, Department of Chemical Engineering, Imperial College London, London SW7 2AZ, UK
[b]Department of Agro-Environmental and Landscape Sciences, University of Bari, Via Orabona 3, 70125 Bari, Italy

Abstract

The performance of organic Rankine cycle (ORC) systems operating in combined heat and power (CHP) mode is investigated. The ORC-CHP systems recover heat from selected industrial waste-heat fluid streams with temperatures in the range 150 °C – 330 °C. An electrical power output is provided by the expanding working fluid in the ORC turbine, while a thermal output is provided by the cooling water exiting the ORC condenser and also by a second heat-exchanger that recovers additional thermal energy from the heat-source stream downstream of the evaporator. The electrical and thermal energy outputs emerge as competing objectives, with the latter favoured at higher hot-water outlet temperatures and *vice versa*. Pentane, hexane and R245fa result in ORC-CHP systems with the highest exergy efficiencies over the range of waste-heat temperatures considered in this work. When maximizing the exergy efficiency, the second heat-exchanger is effective (and advantageous) only in cases with lower heat-source temperatures (< 250 °C) and high heat-delivery/demand temperatures (> 60 °C) giving a fuel energy savings ratio (FESR) of over 40%. When maximizing the FESR, this heat exchanger is essential to the system, satisfying 100% of the heat demand in all cases, achieving FESRs between 46% and 86%.

Keywords: cogeneration; combined heat and power; organic Rankine cycle ; waste-heat recovery; working fluid; thermal energy demand

1. Introduction

The overall efficiency and economic outlook of industrial or urban energy systems can be directly enhanced by utilizing wasted [1] or solar [2] heat, in power generation and/or space heating applications [3]. This is brought to the fore by the fact that (once the heat-recovery infrastructure is in place) no significant further costs are incurred in continuously generating the waste-heat stream that serves as energy input to a suitable heat recovery engine. These engines such as the organic Rankine cycle (ORC) engine [4,5] and the Up-THERM heat converter [6,7] are typically designed to

* Corresponding author. Tel.: +44 (0)20 7594 1442. *E-mail address:* o.oyewunmi@imperial.ac.uk

1876-6102
10.1016/j.egypro.2017.12.557

convert the recovered heat to electrical power or shaft work. The design ORC engines is quite flexible in recovering heat from both low- [8] and high-temperature [9,10] heat sources, with multiple configurations possible [11], and the option of tailoring the working fluid selection to the heat source characteristics [12], including the use of fluid mixtures [13]. Other viable options for waste-heat recovery include the pistonless [14] and the thermoacoustic [15] Stirling engines, the Kalina cycle [16], the Goswami cycle [17] and the NIFTE engines [18,19].

Additional benefits may be realized by serving low-temperature heat demands with the discharged cogenerated heat as in other waste-heat or renewable (*e.g.*, solar) combined heat and power (CHP) applications, thus significantly increasing the global or overall efficiency of the system (*i.e.*, ratio of useful total energy delivered in the form of both heat and electricity to the heat input) [20,21]. While the recovery and reuse of such waste-heat streams in CHP systems has been a topic of discourse amongst researchers, several issues are still under investigation. These include the selection of the system architecture–especially in combination with the ORC system, the choice between conflicting design objectives, the influence of the ORC working fluid and the matching of system output with the thermal demand.

In this paper, we consider waste-heat recovery from three typical flue-gas streams covering a range of temperatures (Table 1) for utilization in an ORC-CHP system wherein shaft/electrical power is generated from the ORC expander, while a thermal output is provided by the cooling stream in the ORC condenser. While an increase in the ORC cooling stream temperature increases the usefulness of the thermal output delivered to the demand, it may also act to reduce the power output [3]. The novelty here is in investigating such conflicting objectives on the system design, including the role of the working fluid. The quality of the thermal output stream is quantified by evaluating its exergy flow-rate increase through the ORC condenser and adding this to the power output to evaluate the overall exergy efficiency of the ORC-CHP system.

Depending on the temperature of the flue gas exiting the evaporator, additional useful exergy can be recovered from it, in a bid to improve the overall exergy efficiency of the ORC-CHP engine. This stream can be used to further satisfy the heat demand [3,22]. In one such arrangement, the hot water is preheated to an intermediate temperature, by the heat rejected in the ORC condenser and then passed through an additional heat exchanger where it extracts heat from this heat source, thereby raising its temperature to the target heat-demand temperature. The option and effectiveness of including this additional heat exchanger in the system is also investigated.

2. System Description

The ORC-CHP systems considered in this work consist of an ORC unit for power generation and a CHP section for space heating in residential and industrial buildings. Heat is recovered from flue gases and transferred to the working fluid in the ORC evaporator, while power is generated by the expansion of the working fluid through a suitable ORC expander (and connected generator). The CHP unit features a two heat-exchanger system wherein heating is provided by the cooling water exiting the ORC condenser. The hot water is initially preheated to an intermediate temperature ($T_{su,int}$) between the cooling water supply temperature (20 °C) and the target hot water supply temperature (T_{su} = 30, 45, 60, 75, 90 °C) by the heat rejected in the ORC condenser. It then passes through an additional heat exchanger (referred to herein as the 'secondary hot-water heater', or SHWH) where it extracts additional heat from this heat source, thereby raising its temperature from the aforementioned intermediate temperature to the target supply temperature. This 'hot' cooling stream is then fed to heating systems in the buildings to provide heat. A schematic diagram of the ORC-CHP system architecture is presented in Fig. 1. It has been assumed that there is 100% heat demand by the consumers.

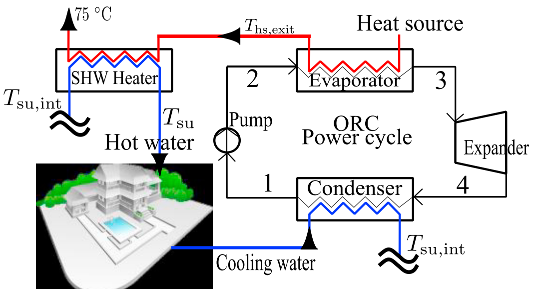

Fig. 1. Schematic of the ORC-CHP system component architecture.

Table 1. Heat source characteristics.

S/N	Heat source type	Temperature	Flowrate
A	High temperature	330 °C	560 kg/s
B	Medium temperature	250 °C	120 kg/s
C	Low temperature	150 °C	30 kg/s

The ORC-CHP system is modelled via energy balances across each component, accounting for the isentropic efficiencies of the pump (85%) and turbo-expander (75%). For the heat exchangers, the energy balance is carried out on both the hot and cold streams, with the assumption of no heat losses in the system, isobaric processes, and with a minimum pinch temperature difference of 10 °C. In addition, the ORC system is kept subcritical. Key performance indicators include the power output from the ORC system ($\dot{W}_{\mathrm{exp}}$), the space-heating exergy ($\dot{E}_{\mathrm{SH}}$), the exergy efficiency and the fuel energy savings ratio (FESR). The FESR is defined as the fuel saved in a CHP plant relative to the fuel needed to meet the separate electrical and heat demands by separate dedicated conventional plants; the electrical efficiency and boiler efficiency values for the conventional plants are taken here to be 40% and 85% respectively. By comparison with the exergy input to the ORC system ($\dot{E}_{\mathrm{in}}$), the exergy efficiency is defined as

$$\eta_{\mathrm{ex}} = \frac{(\dot{W}_{\mathrm{exp}} - \dot{W}_{\mathrm{pump}}) + \dot{E}_{\mathrm{SH}}}{\dot{E}_{\mathrm{in}}}. \tag{1}$$

For the optimization problems, two objectives are investigated, η_{ex} and FESR, and their effects on the configuration of the cycle are monitored. In both optimization problems, constraints are implemented: 1) minimum pinch temperature difference in all heat exchangers is set to 10 °C; 2) minimum temperature of the heat source exiting the system is 75 °C (*i.e.*, its acid dew point); 3) ORC working fluid exits the expander in a superheated state; and 4) condensation pressure is above ambient to avoid sub-atmospheric pressures and expensive solutions to avoid air ingress.

3. Results and Discussion

The performance of the ORC-CHP system is investigated for two settings: 1) maximum exergy efficiency and 2) maximum fuel savings. These optimization studies are carried out for common ORC working fluids, specifically the normal alkanes from butane to octane and the refrigerants R227ea and R245fa, while the effect of the heat delivery/demand temperature (*i.e.*, hot-water supply temperatures between 30 °C and 90 °C) is also investigated.

3.1. Maximizing ORC-CHP exergy efficiency

The maximum exergy efficiency of the ORC-CHP engine and the corresponding net power output from the engine are presented in Fig. 2, both as functions of the hot-water supply temperature (T_{su}), which is varied from 30 °C to 90 °C. For all the heat source types and all the working fluids considered, the exergy efficiency is seen to increase with the T_{su}. In addition, the net power-output generally decreases with the T_{su}. The ORC inlet cooling water is provided at 20 °C, thus higher exit temperatures imply larger temperature gradients across the condenser. This has the tendency of increasing the working fluid condensation temperature and pressure thereby reducing the power output from the ORC expander. There are however some exceptions to this.

For the high temperature heat source, the net power output is constant irrespective of the hot-water supply temperature for hexane, heptane and octane. This is because the condensation takes place at a constant pressure of 1 bar as the cycle is constrained to operate above atmospheric pressure, thus eliminating the need for expensive vacuum expanders and condensers. At this condensation pressure of 1 bar (abs.), the working-fluid temperature is generally greater than the cooling-water exit temperature. For example, the saturation (and condensation) temperatures of heptane and octane at 1 bar are 98 °C and 125 °C, respectively. Thus, increasing the cooling-water exit temperature does not influence the working-fluid condensation temperature and pressure. In addition, due to the high temperature of this heat source (which is higher than the critical temperatures of all the working fluids) and requirement for a subcritical cycle, the optimal evaporation pressure is limited by the critical pressure such that it remains unaffected by the hot-water supply temperature. These keep the power output with these working fluids constant.

Notwithstanding the fact the net power output from the engine generally reduces (save for the above exceptions) with T_{su}, the ORC-CHP system is generally more efficient for designs with higher T_{su}. This indicates that the space-heating/heat-demand potential increases with T_{su}. This increase in heat demand is steeper than the decrease in net power output, leading to an overall increase in the ORC-CHP system's exergy efficiency with the hot-water supply temperature.

From Fig. 2 it is clear that in butane, R245fa and R227ea cycles the exergy efficiency decreases with the heat-source temperature; the efficiencies are lower in the low-temperature heat source cases and highest in the high-temperature case. This result can be linked to the critical temperatures of these fluids and the fact that the cycles are subcritical. Butane, R245fa and R227ea have low critical temperatures and the subcritical nature of the system limits the evaporation temperature/pressure to a constant value as the heat-source/heat-addition temperature is increased. Thus, there is a larger average temperature difference between the heat source and the working fluids. This leads to larger exergy destruction in the evaporator, resulting in the lower exergy efficiencies at higher heat source temperatures. Other fluids such as hexane, heptane and octane are not limited in this way and the efficiency of their cycles increases with the heat source temperature.

However, the efficiencies for cycles with pentane reach a maximum at the medium heat-source temperature and decrease thereafter. This also follows from the critical temperature and subcritical cycle correlation. Between the medium- and high-temperature heat sources, the evaporation temperature is constant, resulting in a larger temperature difference between heat source and working fluid, leading to higher exergy destruction and hence the lower exergy efficiency.

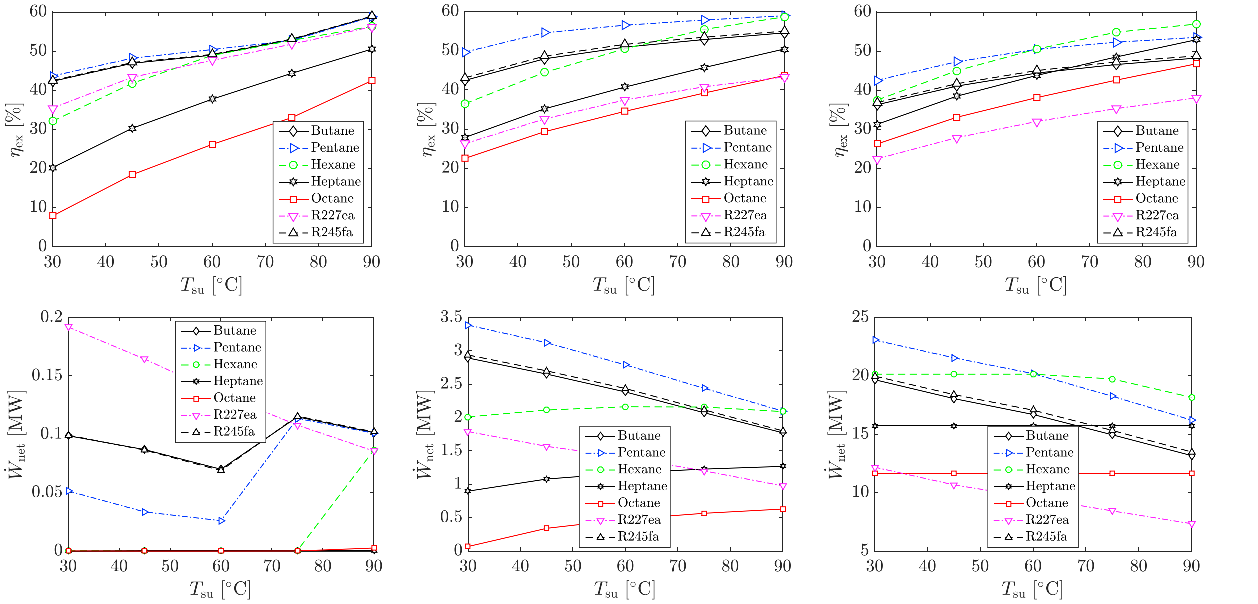

Fig. 2. Maximum exergy efficiency and corresponding net power output of the ORC-CHP engine with various working fluids for each case study (LHS: low-temperature, middle: medium-temperature, RHS: high-temperature heat source), as a function of the hot-water supply temperature.

3.2. Addition of SHWH heat exchanger

It is expected that the overall efficiency of the ORC-CHP system should improve by the inclusion of the SHWH that further recovers heat from the waste-heat source for hot-water production. The amount of useful exergy obtainable from the heat source after the evaporator is a direct function of the temperature of the heat source exiting the evaporator ($T_{hs,exit}$) and also its mass flow rate. As the heat sources considered are flue gases, the exergy is limited by the acid dew point of the gas (estimated as 75 °C). If $T_{hs,exit}$ is greater than this dew point temperature, then the SHWH can serve to improve the efficiency of the system. In such a case, the ORC cooling water needs to exit the condenser at a temperature ($T_{su,int}$) lower than the heat demand temperature (T_{su}) and the heat source, via the SHWH, provides the additional heat to attain the required T_{su}. Thus, the heat demand is provided by the ORC condenser and the SHWH. If $T_{hs,exit}$ is not greater than the dew point temperature, then the heat demand is satisfied by the ORC condenser (raising the temperature of the ORC cooling stream from 20 °C to $T_{su,int} = T_{su}$) alone and there is no need for the SHWH.

The temperature enthalpy (T–$\dot{Q}$) diagrams of the ORC power cycle for the three heat sources (with pentane as the working fluid) are presented in Fig. 3 where it is seen that the heat-source exit temperatures are lowest for the high-temperature heat source and highest for the low-temperature heat source. In the low-temperature case, the working fluid is evaporated at low temperatures/pressure, causing the evaporator pinch to occur at the onset of evaporation and leading to the low temperature drop in the heat source and high $T_{hs,exit}$. For the high- and medium-temperature heat sources, the combination of the higher source temperatures and the subcritical imposition, causes $T_{hs,exit}$ to be quite low. As a matter of fact, for the high-temperature heat source, $T_{hs,exit}$ = 75 °C in all instances for all the working fluids and for all T_{su}, thus $T_{su,int}$ = T_{su} (always, and not just for pentane in Fig. 3, RHS) and since no additional heat can be extracted from the heat source, the SHWH (and the associated capital expenditure) is not required here.

However, for low-temperature heat sources (and in some instances, medium-temperature sources), this SHWH will be required to further reduce the temperature of the heat source stream and improve the efficiency of the system; this benefit is more evident for the cases with high hot-water supply temperatures (60 °C, 75 °C and 90 °C). The intermediate temperatures in these cases are given in Table 2, where the fraction of the heat demand provided by the SHWH ($\dot{Q}_{HW,frac}$) is also provided, for all the working fluids at heat demand temperatures of 60 °C, 75 °C and 90 °C. When T_{su} = 60 °C, it is only in the system with the low-temperature heat source and R227ea as working fluid, that the SHWH provide a substantial part of the heat demand (9.2%). At higher values of T_{su} however, the SHWH is seen to be more effective, providing between 22% and 60% (and 100% in the case of the system with the low-temperature heat source and octane as working fluid) of the heat demand. Thus, for ORC-CHP systems with low heat-source temperatures and in which high hot-water supply temperatures are desired, this alternative system configuration with a SHWH is worth investigating.

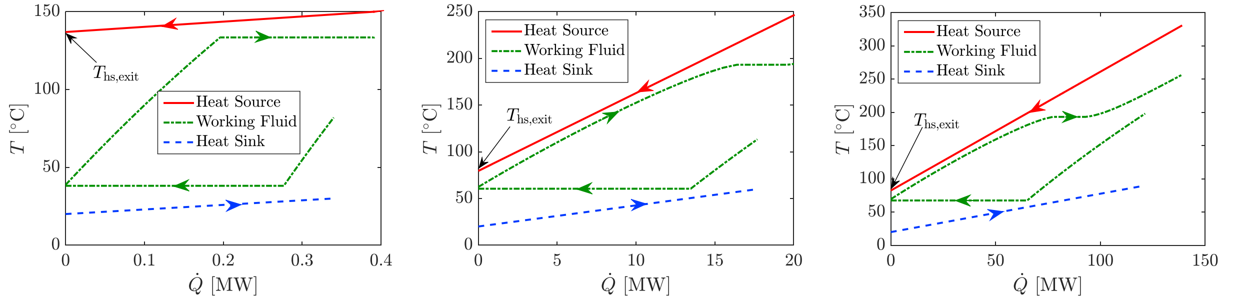

Fig. 3. T–$\dot{Q}$ diagrams of the ORC evaporator and condenser with pentane as the working fluid. LHS: the low-temperature heat source and T_{su} = 30 °C; MIDDLE: the medium-temperature heat source and T_{su} = 60 °C; RHS: the high-temperature heat source and T_{su} = 90 °C.

Table 2. The intermediate temperatures ($T_{su,int}$) of the hot water stream between the condenser and the SHWH for the ORC-CHP system operating on the low-temperature and medium-temperature heat sources, at final hot-water supply temperatures of 60 °C, 75 °C and 90 °C. The fraction of heat demand fulfilled by the SHWH ($\dot{Q}_{HW,frac}$) is also provided.

Working fluids	Low-temperature heat source						Medium-temperature heat source					
	60 °C	75 °C	90 °C	60 °C	75 °C	90 °C	60 °C	75 °C	90 °C	60 °C	75 °C	90 °C
	$T_{su,int}$ (°C)			$\dot{Q}_{HW,frac}$ (%)			$T_{su,int}$ (°C)			$\dot{Q}_{HW,frac}$ (%)		
Butane	60.0	51.7	56.4	0.0	51.7	56.0	59.7	72.6	89.6	0.9	5.4	0.6
Pentane	60.0	50.6	55.1	0.0	54.3	58.2	59.0	71.0	82.2	3.4	8.8	12.9
Hexane	60.0	75.0	61.7	0.0	0.0	47.2	60.0	73.1	73.9	0.0	4.2	26.8
Heptane	60.0	75.0	90.0	0.0	0.0	0.0	60.0	75.0	90.0	0.0	0.0	0.0
Octane	60.0	75.0	30.0	0.0	0.0	100	60.0	75.0	90.0	0.0	0.0	0.0
R227ea	57.2	65.0	65.0	9.2	22.2	41.7	60.0	75.0	82.0	0.0	0.0	13.4
R245fa	60.0	51.7	56.3	0.0	51.7	56.1	60.0	72.6	90.0	0.1	5.4	0.0

3.3. Maximum FESR and effect on SHWH

The fuel energy savings ratio (FESR) is a CHP performance indicator that demonstrates the benefits of a CHP system relative to a combination of a conventional power station and boiler. Conventional power plants are more efficient than ORC power systems due to the low temperature of the ORC waste-heat source, thus positive FESR values are enhanced by generating large amounts (or high temperature) of hot water to satisfy heat demand. The FESR of the ORC-CHP system is presented in Fig. 4. At hot-water supply temperatures (T_{su}) below 45 °C, the system has negative FESR as little or no heat demand is catered for, and its electrical efficiency is generally lower than the 40% assumed for the conventional plant. However, at higher supply temperatures, larger amounts of heating capacity are provided, and the ORC-CHP system is seen to perform favourably in comparison to the conventional systems with FESR values in excess of 10%.

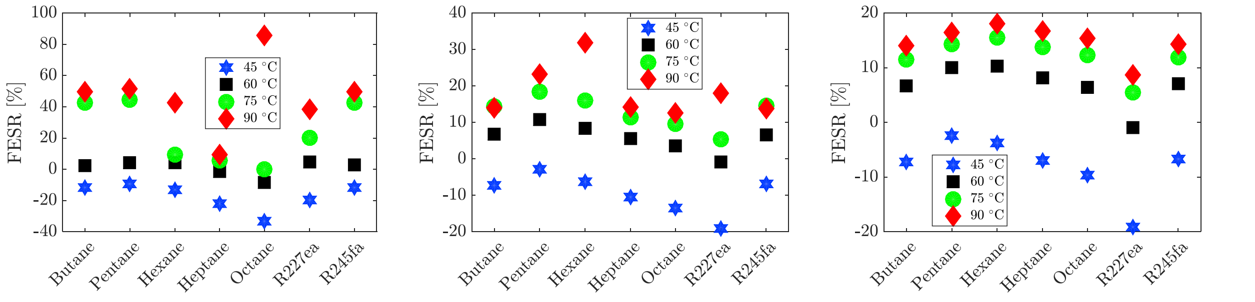

Fig. 4. The fuel-energy savings ratio (FESR) of the ORC-CHP engine at maximum exergy efficiency for each case study (LHS: low-temperature, middle: medium-temperature, RHS: high-temperature heat source), at hot-water supply temperatures of 45 °C, 60 °C, 75 °C and 90 °C.

At lower heat source temperatures, the FESR of the system is seen to increase considerably in comparison to the high-temperature heat source. This is a direct result of the engine generating more heating capacity relative to the electric power. This can be measured by the heat-to-power ratio (HPR) of the engine for the three heat sources. For the high-temperature heat source, (working fluid) average HPR ranges from 4.5 (T_{su} = 45 °C) to 7.5 (T_{su} = 90 °C) while the HPR ranges from 4.8 to 8.8 for the medium-temperature heat source. For the low-temperature heat source, it ranges from 6.1 to 18.4 (excluding octane); it ranges from 23 to 40 for octane at the low-temperature heat source.

When the problem is redefined to the maximization of the FESR, the system is seen to favour meeting the heat demand requirements, with very low power production. This is in line with the definition of the FESR; electric power production from the CHP engine is less efficient than from a conventional plant thus maximizing the FESR tends to increase the systems heating capacity to the maximum possible (within feasibility of constraints), while reducing the power output. The results of maximizing the FESR are presented in Table 3, where the averages for all considered working fluids are reported. The corresponding exergy efficiencies and the power output from the cycle, for the representative case of the medium-temperature heat source, are presented in Fig. 5.

Table 3. Average maximum FESR values (%) for the three heat-source cases at heat delivery temperatures from 45 °C to 90 °C. The maximum deviation across the working fluids is ± 1.57% (abs.) at 45 °C and ± 0.03% (abs.) at other temperatures.

T_{su} (°C)	Low	Medium	High
45	45.5	46.2	46.2
60	71.7	71.7	71.7
75	81.1	81.1	81.1
90	85.8	85.9	85.9

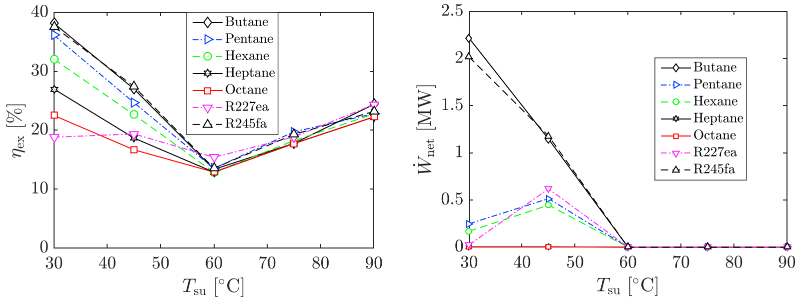

Fig. 5. Exergy efficiency and net power output of the ORC-CHP system with the medium-temperature heat source, at maximum FESR, as a function of the hot-water supply temperature.

The power produced and exergy efficiency are generally less than the scenario wherein the exergy efficiency is maximized. At T_{su} < 60 °C, the power output decreases with increasing T_{su}, and the efficiency mirrors this trend, whereas at higher T_{su}, the power output is negligible and the exergy efficiency increases due the larger amount and higher quality of hot water generated. This low power and high heat capacity setting, leads to very high heat-to-power ratio (> 1000) as increases in FESR are mainly influenced by increases in the heat energy generated.

Furthermore, maximizing the FESR results in the SHWH handling all the heat demand requirements (*i.e.*, 100% in comparison to the figures in Table 2); this applies to all heat source cases, all heat demand temperatures and all working fluids. From Table 3, at the same heat source and heat demand conditions, the working fluids are seen to have very similar FESR as very low deviations from the average are recorded. Thus, the problem of maximizing the FESR focusses on the heat exchange between the waste-heat stream and the cooling-water stream in the SHWH, with minimum power production from the ORC power cycle. Hence, it can be concluded that the maximum FESR depends on the external system conditions and is insensitive to the choice of working fluid.

4. Conclusions

The performance of an ORC-CHP system when utilizing waste-heat from industrial processes is evaluated with respect to the system's net power-output, heat-delivery energy/exergy available in the cooling-water stream (hot-water covering a heat demand), fuel energy savings ratio (FESR), and overall exergy efficiency. Flue-gas streams with temperatures ranging from 150 °C to 330 °C are considered as the heat source for this system. Power production and heat delivery are generally in competition, with the heat-delivery exergy increasing and the power output decreasing when the heat-demand temperature is higher within a range of temperatures from 30 °C to 90 °C. Pentane, hexane and R245fa are among the best performing working fluids, resulting in cycles with the highest efficiencies across the heat source temperatures considered. When the exergy efficiency is maximized, the additional heat exchanger (the SHWH) is seen to be rarely effective; for systems with high heat source temperatures, this heat exchanger can be neglected. At medium and lower heat source temperatures, the SHWH improves the overall efficiency of the system when the heat demand temperatures are greater than 60 °C, with the heat exchanger delivering over 50% of the required heat demand load especially at low heat source temperatures and high heat demand temperatures. The FESR in comparison to conventional power plants and boilers is found here to range from -20% (at low heat-delivery temperatures) to over 40% (at higher heat-delivery temperatures and lower heat-source temperatures). However, on maximizing the FESR, the SHWH features more prominently, delivering 100% of the required heat demand in all cases, as is seen to favour meeting the heat demand requirements, with very low power production. The FESR values are also seen to be much higher than when the exergy efficiency of the system is maximized. The maximum FESR ranges between 46% and 86% at low and high heat demand temperatures respectively. In addition, at similar heat source and heat demand temperatures, the FESR shows very little deviation among the working fluids considered (maximum of ±1.57%, absolute) from which it is concluded that the maximum FESR is insensitive to the choice of working fluid but only depends on the external conditions, *i.e.*, the heat source and heat demand temperatures.

Acknowledgements

This work was supported by the UK Engineering and Physical Sciences Research Council (EPSRC) [grant number EP/P004709/1]. Data supporting this publication can be obtained on request from cep-lab@imperial.ac.uk.

References

[1] Markides CN. The role of pumped and waste heat technologies in a high-efficiency sustainable energy future for the UK. Appl Therm Eng 2013;53 (2):197–209.
[2] Markides CN. Low-concentration solar-power systems based on organic Rankine cycles for distributed-scale applications: Overview and further developments. Front Energy Res 2015;3:47.
[3] Oyewunmi OA, Kirmse CJW, Pantaleo AM, Markides CN. Performance of working-fluid mixtures in ORC-CHP systems for different heat-demand segments and heat-recovery temperature levels. Energy Convers Manag 2017;148: 1508–24.
[4] Oyewunmi OA, Taleb AI, Haslam AJ, Markides CN. On the use of SAFT-VR Mie for assessing large-glide fluorocarbon working-fluid mixtures in organic Rankine cycles. Appl Energy 2016;163:263–82.
[5] Oyewunmi OA, Taleb AI, Haslam AJ, Markides CN. An assessment of working-fluid mixtures using SAFT-VR Mie for use in organic Rankine cycle systems for waste-heat recovery. Comput Therm Sci 2014;6:301–16.
[6] Kirmse CJW, Oyewunmi OA, Taleb AI, Haslam AJ, Markides CN. Two-phase single-reciprocating-piston heat conversion engine: Non-linear dynamic modelling. Appl Energy 2017;186:359–75.
[7] Oyewunmi OA, Kirmse CJW, Haslam AJ, Müller EA, Markides CN. Working-fluid selection and performance investigation of a two-phase single-reciprocating-piston heat-conversion engine. Appl Energy 2017;186:376–95.
[8] Tchanche BF, Lambrinos G, Frangoudakis A, Papadakis G. Low-grade heat conversion into power using organic Rankine cycles – A review of various applications. Renew Sustain Energy Rev 2011;15(8):3963–79.
[9] Lai NA, Wendland M, Fischer J. Working fluids for high-temperature organic Rankine cycles. Energy 2011;36(1):199–211.
[10] Kirmse CJW, Oyewunmi OA, Haslam AJ, Markides CN. Comparison of a novel organic-fluid thermofluidic heat converter and an organic Rankine cycle heat engine. Energies 2016;9(7):47.
[11] Lecompte S, Huisseune H, van den Broek M, Vanslambrouck B, De Paepe M. Review of organic Rankine cycle (ORC) architectures for waste heat recovery. Renew Sustain Energy Rev 2015;47:448–61.
[12] White MT, Oyewunmi OA, Haslam AJ, Markides CN. Industrial waste-heat recovery through integrated computer-aided working-fluid and ORC system optimisation using SAFT-γ Mie. Energy Convers Manag 2017; https://doi.org/10.1016/j.enconman.2017.03.048
[13] Oyewunmi OA, Markides CN. Thermo-economic and heat transfer optimization of working-fluid mixtures in a low-temperature organic Rankine cycle system. Energies 2016;9(6):448.
[14] Ceperley PH. A pistonless Stirling engine—the traveling wave heat engine. J Acoust Soc Am 1979;66(5):1508–13.
[15] Backhaus S, Swift GW. A thermoacoustic Stirling heat engine. Nature 1999;399(6734):335–8.
[16] Kalina AI, Tribus M. Advances in Kalina cycle technology 1980-1991: Part I: Development of a practical cycle, 1992.
[17] Goswami DY, Solar thermal power technology: Present status and ideas for the future, Energy Sources 1998;20(2):137–145.
[18] Markides CN, Solanki R, Galindo A, Working fluid selection for a two-phase thermofluidic oscillator: Effect of thermodynamic properties, Appl Energy 2014;124:167–185.
[19] Markides CN, Smith TCB. A dynamic model for the efficiency optimization of an oscillatory low grade heat engine. Energy 2011;36(12):6967–80.
[20] Freeman J, Hellgardt K, Markides CN. An assessment of solar-powered organic Rankine cycle systems for combined heating and power in UK domestic applications. Appl Energy 2015;138:605–20.
[21] Dong L, Liu H, Riffat S. Development of small-scale and micro-scale biomass-fuelled CHP systems – A literature review. Appl Therm Eng 2009;29(11):2119–26.
[22] Habka M, Ajib S. Performance estimation of mixtures in solar Organic Rankine Cycle with two mini cogeneration options for improvement purpose. Sustain Energy Technol Assess 2016;16:174–89.